Z. Phys. C – Particles and Fields 44, 365–378 (1989)

Zeitschrift für Physik C Particles and Fields

Production and decay of charmed mesons in $e^+ e^-$ annihilation at $\sqrt{s} > 28$ GeV

TASSO Collaboration

W. Braunschweig, R. Gerhards, F.J. Kirschfink[1], H.-U. Martyn
I. Physikalisches Institut der RWTH, D-5100 Aachen, Federal Republic of Germany[a]

H.M. Fischer, H. Hartmann, J. Hartmann, E. Hilger, A. Jocksch, R. Wedemeyer
Physikalisches Institut der Universität, D-5300 Bonn, Federal Republic of Germany[a]

B. Foster, A.J. Martin
H.H. Wills Physics Laboratory, University of Bristol, Bristol, UK[b]

E. Bernardi[2], J. Chwastowski[3], A. Eskreys[3], K. Gather, K. Genser[4], H. Hultschig, P. Joos, H. Kowalski[5], A. Ladage, B. Löhr, D. Lüke[6], P. Mättig[7], D. Notz, J.M. Pawlak[4], K.-U. Pösnecker, E. Ros, D. Trines, R. Walczak[4], G. Wolf
Deutsches Elektronen-Synchrotron DESY, D-2000 Hamburg, Federal Republic of Germany

H. Kolanoski
Physikalisches Institut, Universität Dortmund, Federal Republic of Germany[a]

T. Kracht[8], J. Krüger, E. Lohrmann, G. Poelz, W. Zeuner[9]
II. Institut für Experimentalphysik der Universität, D-2000 Hamburg, Federal Republic of Germany[a]

R.S. Galik[10], J. Hassard, J. Shulman, D. Su[11], I. Tomalin, A. Watson
Department of Physics, Imperial College, London SW7 2AZ, UK[b]

F. Barreiro, A. Leites, J. del Peso
Universidad Autonoma de Madrid, E-Madrid, Spain[c]

M.G. Bowler, P.N. Burrows[11], M.E. Veitch
Department of Nuclear Physics, Oxford University, Oxford OX1 3RH, UK[b]

G.E. Forden[12], J.C. Hart, D.H. Saxon
Rutherford Appleton Laboratory, Chilton, Didcot, Oxon OX11 0QX, UK[b]

S. Brandt, M. Holder
Fachbereich Physik der Universität-Gesamthochschule, D-5900 Siegen, Federal Republic of Germany[a]

Y. Eisenberg, U. Karshon, G. Mikenberg, A. Montag, D. Revel, E. Ronat, A. Shapira, N. Wainer, G. Yekutieli
Weizmann Institute, Rehovot 76100, Israel[d]

A. Caldwell[13], D. Muller[14], S. Ritz[13], D. Strom[15], M. Takashima[9], Sau Lan Wu, G. Zobernig
Department of Physics, University of Wisconsin, Madison, WI 53706, USA[e]

Received 11 May 1989

[1] Now at Lufthansa, Hamburg, FRG
[2] Now at Robert Bosch GmbH, Schwieberdingen, FRG
[3] Now at Inst. of Nuclear Physics, Cracow, Poland
[4] Now at Warsaw University[f], Poland
[5] On leave at Columbia University, NY, USA
[6] On leave at CERN, Geneva, Switzerland
[7] Now at IPP Canada, Carleton University, Ottawa, Canada
[8] Now at Hasylab, DESY, Hamburg, FRG
[9] Now at CERN, Geneva, Switzerland
[10] Permanent address Wilson Lab., Cornell Univ., Ithaca, NY, USA
[11] Now at MIT, Cambridge, MA, USA
[12] Now at SUNY Stony Brook, Stony Brook, NY, USA
[13] Now at Columbia University, NY, USA
[14] Now at SLAC, California, CA, USA
[15] Now at University of Chicago, Chicago, IL, USA

[a] Supported by Bundesministerium für Forschung und Technologie
[b] Supported by UK Science and Engineering Research Council
[c] Supported by CAICYT
[d] Supported by the Minerva Gesellschaft für Forschung GmbH
[e] Supported by US Dept. of Energy, contract DE-AC02-76ER000881 and by US Nat. Sci. Foundation Grant no INT-8313994 for travel
[f] Partially supported by grant CPBP 01.06

Abstract. We report on a study of inclusive production of $D^{*\pm}$ mesons in e^+e^- annihilation at c.m. energies between 28 and 46.8 GeV using the TASSO detector at the PETRA storage ring. A hard $D^{*\pm}$ energy spectrum is measured with a maximum near $E_{D^{*\pm}} \simeq 0.6 E_{\text{beam}}$. The measured cross section ratio $(\sigma_{D^{*+}} + \sigma_{D^{*-}})/\sigma_{\mu\mu} = 1.28 \pm 0.09 \pm 0.18$ indicates that D^* production accounts for a large fraction of the observed charm production. Two complementary methods have been used to determine the forward-backward asymmetry of charm pair production due to electroweak interference. Combining both measurements the product of the axial vector couplings of the electron and the charm quark to the weak neutral current was determined to be $g_A^e g_A^c = -(0.276 \pm 0.073)$, in agreement with the standard model prediction of -0.25. Using a sample of reconstructed $D^{*\pm}$ mesons, the relative strength of the strong interaction coupling of the c quark compared to that of an average of all flavours is measured as $\alpha_s(c)/\alpha_s(all) = 0.91 \pm 0.38 \pm 0.15$, consistent with the coupling constant being flavour independent. An update of our D^0 lifetime measurement is presented, based on a considerable increase in statistics, the final result being $\tau_{D^0} = (4.8^{+1.0+0.5}_{-0.9-0.7}) 10^{-13}$ s.

1 Introduction

The formation of hadrons in e^+e^- annihilation predominantly proceeds via quark-pair production, $e^+e^- \to q\bar{q}$, with the quark and the antiquark subsequently fragmenting into the observed particles. While the production process is calculable in perturbative QCD, the hadronisation has not yet been understood in a similar fashion. A study of the quark fragmentation distributions, which describe the dynamical mechanism by which quarks transform into jets of hadrons, is therefore of special interest.

In the case of light quarks u, d, and s the detection of the final state hadron which carries the primary quark or antiquark is rather difficult since many of these quarks are produced during the fragmentation process. The situation is completely different in the case of a heavy quark such as charm or bottom. A charmed hadron carrying a large fraction of the beam energy will in general contain the primary charm quark produced in the hard scattering process since *i*) the production rate of charmed (or heavier) quarks during the fragmentation is exceedingly small at present energies and *ii*) charmed hadrons originating from the decay of bottom hadrons have comparatively low momenta. The measurement of the inclusive differential cross section of such charmed hadrons provides a clean way of studying charm fragmentation.

Because of their clear signature the charmed vector mesons $D^{*\pm}$ form a particularly good laboratory to analyse the characteristics of charm quark production and fragmentation in high energy e^+e^- annihilation. Reconstructing $D^{*\pm}$ mesons has by now become a well known technique which has been employed previously by many experiments [1–11], including TASSO [12–15].

Comparing the total cross section for $e^+e^- \to D^{*\pm} X$ with the production rate of the pseudoscalar mesons $D^\pm$ and D^0, $\bar{D}^0$, the influence of the spin (and the quark masses) on the hadronisation can be investigated. From simple spin-counting arguments one expects that vector mesons are produced three times as often as pseudoscalar mesons. Since the masses of the D^* and the D mesons are almost equal ($M_{D^*}/M_D \sim 1.07$) this naive argument should still be valid in the charm sector.

In the standard model the e^+e^- annihilation into quark pairs at PETRA energies proceeds predominantly via a time-like virtual photon with a small contribution from Z^0 exchange. The interference of the electromagnetic and the weak current is expected to show up most significantly as a forward-backward asymmetry in the production angular distribution of the charm quark.

The flavour independence of the strong coupling constant α_s can be best tested by measuring the ratio $\alpha_s(q)/\alpha_s(all)$ for different flavours, thus cancelling most of the systematic effects. In an earlier publication we determined this ratio for charm quarks by considering event shape variables like thrust and sphericity [14]. To reduce systematic effects of the jet definition and of the fragmentation process, we use the asymmetry of the energy-energy correlation (EEC) for this measurement.

The paper is organised as follows. First we briefly describe in Sect. 2 and 3 the data sample on which the analysis is based and the selection criteria to reconstruct $D^{*\pm}$ mesons. In Sect. 4 the measurement of the differential and total cross sections for inclusive $D^{*\pm}$ meson production is presented. Section 5 reports the measurement of the charm quark asymmetry, using both reconstructed $D^{*\pm}$ mesons and a method that tags $D^{*\pm}$ mesons via the low momentum pion from the decay $D^{*\pm} \to D^0(\bar{D}^0)\pi^\pm$. In Sect. 6 we present a determination of the ratio of coupling constants $\alpha_s(c)/\alpha_s(all)$. An improved measurement of the D^0 meson lifetime is described in Sect. 7 and our results are summarized in Sect. 8.

2 Data sample

The experiment was carried out using the TASSO detector at the PETRA storage ring at DESY. A detailed description of the detector can be found in [16, 17]. The data were collected at centre of mass energies between 28 GeV and 46.8 GeV (the highest energy reached at PETRA), the average being 36.2 GeV. A total of 62,152 events from e^+e^- annihilation into hadrons were selected following a method described in [17, 18], roughly 10 percent taken at energies above 40 GeV, and the bulk of the data around 35 GeV. The corresponding integrated luminosity amounted to $\int L dt = 234\,\mathrm{pb}^{-1}$. It should be noted that the data sample includes the events of the previous analyses [12–15]. The measurement of the D^0 lifetime is based on a smaller subsample of events recorded after the installation of a high resolution vertex chamber in 1982 [19].

In this analysis only charged particles were used. The momentum resolution was improved by using the average beam position in constrained track fitting, yielding $\sigma_p/p = 0.010\sqrt{2.9+p^2}$ (p in GeV/c) [12] for tracks going out perpendicular to the beam axis.

3 Selection of $D^{*\pm}$ candidates

The D^{*+} mesons were identified using the decay

$$D^{*+} \to D^0 \pi_s^+ \tag{1}$$

where here and henceforth only the particle states are indicated; the analysis includes also the charge conjugate states. The D^{*+} were isolated exploiting the special decay kinematics due to the fact that the Q-value of reaction (1) is only 5.8 MeV [20, 21], giving the soft pion (π_s) a maximum transverse

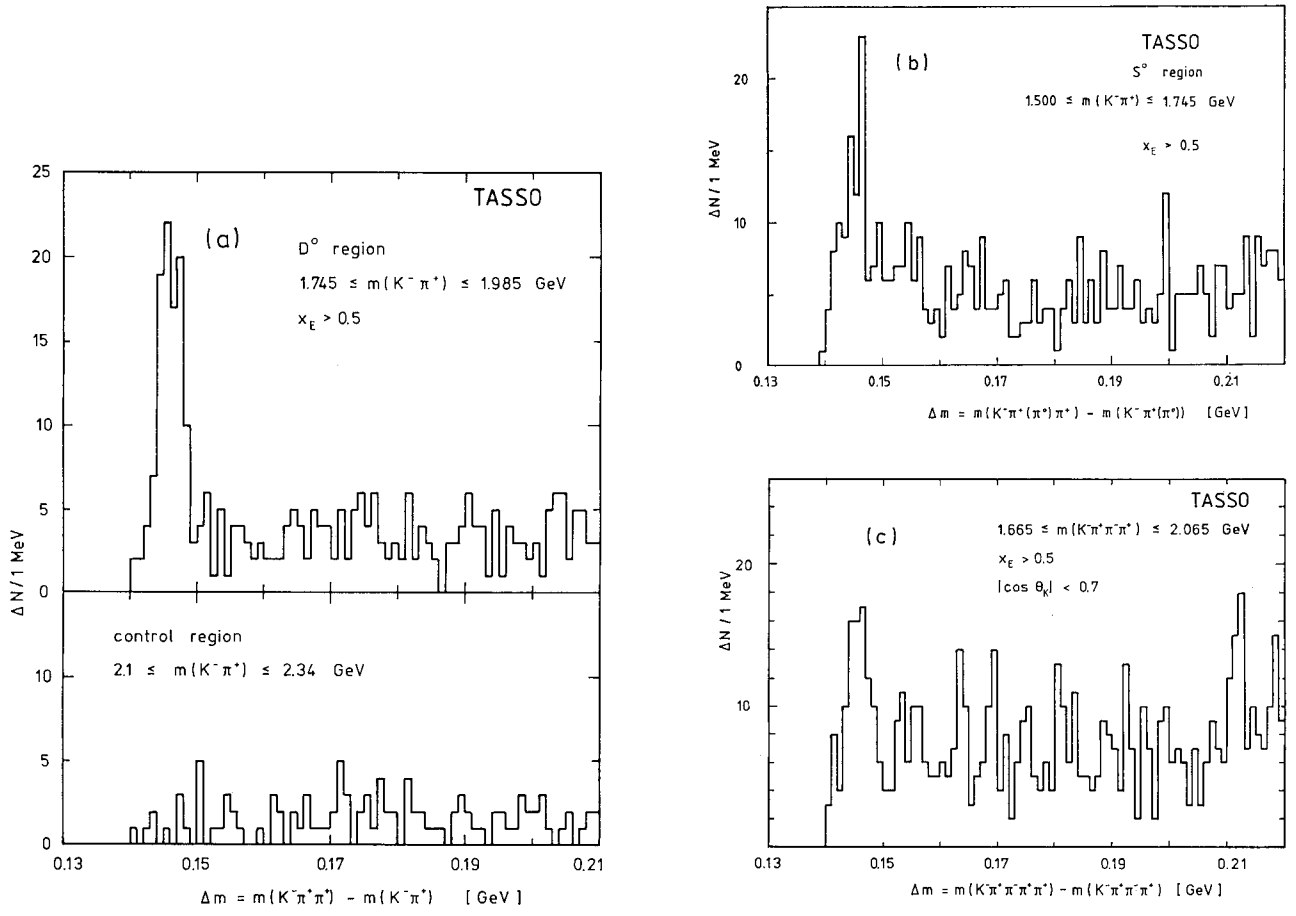

Fig. 1. a Distribution of the mass difference $\Delta M = M(K^-\pi^+\pi^+) - M(K^-\pi^+)$ for combinations with $x_E > 0.5$ and $|M(K^-\pi^+) - M(D^0)| < 0.12$ GeV. Also shown is the mass difference distribution for combinations with $x_E > 0.5$ in the control region 2.10 GeV $< M(K^-\pi^+) <$ 2.34 GeV. **b** Distribution of the mass difference $\Delta M = M(K^-\pi^+\pi^+) - M(K^-\pi^+)$ for combinations with $x_E > 0.5$ and 1.50 GeV $< M(K^-\pi^+) <$ 1.745 GeV. **c** Distribution of the mass difference $\Delta M = M(K^-\pi^+\pi^-\pi^+\pi^+) - M(K^-\pi^+\pi^-\pi^+)$ for combinations with $x_E > 0.5$ and $|M(K^-\pi^+\pi^-\pi^+) - M(D^0)| < 0.12$ GeV

momentum of $p_T = 39.6$ MeV/c with respect to the D^{*+} line of flight. Hence a reduction of the combinatorial background and a better resolution is expected in the distribution of the *mass difference*

$$\Delta M = M(D^0\pi^+) - M(D^0) \quad (2)$$

rather than in the D^{*+} mass distribution itself, whose width is dominated by the limited momentum resolution of the detector. The D^0 meson was searched for in the decay channels

$$D^0 \to K^-\pi^+ \quad (3)$$

$$\to K^-\pi^+(\pi^0) \quad (4)$$

$$\to K^-\pi^+\pi^-\pi^+. \quad (5)$$

For each event all possible $M(K^-\pi^+)$ and $M(K^-\pi^+\pi^-\pi^+)$ mass combinations were calculated using charged tracks with momenta $p > 0.8$ GeV/c. No particle identification has been used in the analysis; each particle was assumed to be a kaon or pion. All track momenta were corrected for energy loss in the beampipe. The mass distributions have no obvious structure in the D^0 mass region. Those combinations which lay within 0.120 GeV and 0.200 GeV of the nominal D^0 mass of 1.865 GeV were ascribed to reactions (3) and (5), respectively, and were combined with an additional charged track to test for reaction (1). The π_s was required to have a momentum greater than 0.3 GeV/c.

To reduce the combinatorial background in reaction (5) we imposed two further requirements on the candidate events: *i*) all particles, including the soft pion, were required to lie within the same event hemisphere, defined with respect to the sphericity axis, and *ii*) the decay angle of the D^0 in its helicity frame had to fulfil $|\cos\theta_K^*| < 0.7$ (θ_K^* is the angle between the K^- and the D^0 momenta in the D^0 rest frame).

For the $K^-\pi^+\pi^0$ decay mode of the D^0 (reaction (4)), no attempt was made to reconstruct the π^0 explicitly. Instead the well known kinematic enhancement in the $M(K^-\pi^+)$ mass spectrum around 1.6 GeV, called the 'S^0' peak [22], was used, which is understood to result from the decay sequences $D^0 \to K^-\rho^+ \to K^-\pi^+\pi^0$ and $D^0 \to K^{*-}\pi^+ \to K^-\pi^0\pi^+$, the π^0 not being detected. The S^0 mass region was defined as $1.50\ \text{GeV} < M(K^-\pi^+) < 1.745$ GeV.

The D^{*+} production has been analysed in terms of its fractional energy x_E, defined as

$$x_E = \frac{E_{D^{*+}}}{E_{\text{beam}}},$$

where E_{beam} denotes the beam energy.

Figure 1a to c shows the distributions of the mass difference (2) for the three decay modes (3) to (5) with $x_E > 0.5$. In all channels clear evidence for D^{*+} production is found as distinct enhancements of 106, 106, and 101 combinations, respectively, in the signal region, defined as $\Delta M < 0.15$ GeV. The observed widths are in agreement with the mass resolutions as obtained from a Monte Carlo calculation. No enhancement is observed if instead the mass $M(K^-\pi^+)$ is required to be in the control region $2.10\ \text{GeV} < M(K^-\pi^+) < 2.34$ GeV, far above the D^0 mass, as shown for example for reaction (3) in Fig. 1a. For reaction (3) the mass region below the D^0 cannot be used because of the S^0 satellite enhancement.

4 Cross section for inclusive D^{*+} production

To measure the differential cross section for D^{*+} production, which is known to be peaked at high x_E values, the data of decay channels (3) and (5) have been utilized. For the region $0.2 \leqq x_E \leqq 0.4$, which is close to the threshold of $x_E = 0.117$, only reaction (3) could be used. The background in this region was reduced by requiring $|\cos\theta_K^*| < 0.7$, where θ_K^* is defined as above.

Table 1. Differential cross sections for $D^{*\pm}$ production. N, ΔN are the number of events and their statistical uncertainties, respectively, ε_{D^*} denotes the efficiency to detect a $D^{*\pm}$ candidate in the given decay mode for accepted hadronic events

$D^{*+} \to D^0\pi^+ \to K^-\pi^+\pi^+$

x_E	$N \pm \Delta N$	ε_{D^*}	$\frac{d\sigma}{dx}$ [10^{-3} nb]	$\frac{s}{\beta}\frac{d\sigma}{dx}$ [μb GeV^2]
0.2–0.3	2.8±1.7	0.14	46±28	68±41
0.3–0.4	16.5±4.1	0.35	109±27	150±37
0.4–0.5	21.1±4.6	0.42	116±25	157±34
0.5–0.6	29.0±5.4	0.42	178±31	238±42
0.6–0.7	34.2±5.8	0.35	226±38	300±51
0.7–0.8	17.6±4.2	0.29	140±33	186±44
0.8–1.0	11.4±3.4	0.28	47±14	62±19

$D^{*+} \to D^0\pi^+ \to K^-\pi^+\pi^-\pi^+\pi^+$

x_E	$N \pm \Delta N$	ε_{D^*}	$\frac{d\sigma}{dx}$ [10^{-3} nb]	$\frac{s}{\beta}\frac{d\sigma}{dx}$ [μb GeV^2]
0.4–0.5	25.0±5.0	0.18	153±31	219±41
0.5–0.6	34.0±5.8	0.17	221±38	296±50
0.6–0.7	18.5±4.3	0.15	136±32	181±42
0.7–0.8	10.0±3.2	0.13	85±27	113±36
0.8–1.0	5.5±2.3	0.13	23±10	31±13

To determine the number of D^{*+} mesons per x_E interval a background subtraction has been performed for each bin separately. The background shape was estimated from a large sample of Monte Carlo events, using the upper D^0 side band. The background fraction was calculated by normalising this Monte Carlo shape to the ΔM region 0.16 GeV $< \Delta M <$ 0.20 GeV and then extrapolating to the signal region $\Delta M <$ 0.15 GeV. The Monte Carlo events were generated using the Lund Monte Carlo program (version 6.2) [23], and tracing the events through a full simulation of the TASSO detector and through the same analysis chain as the real data. The same Monte Carlo program was used to calculate the efficiency for detecting the D^{*+} mesons (see Table 1), as well as the event acceptance and radiative corrections.

The main uncertainty in determining the cross section comes from the errors in the branching ratios for the observed decay modes. For the relevant branching ratios we used the values recently published by the Particle Data Group [24], namely $B(D^0 \to K^- \pi^+) = (3.77^{+0.37}_{-0.32})\%$, $B(D^0 \to K^- \pi^+ \pi^- \pi^+) = (7.9^{+1.0}_{-0.9})\%$, and $B(D^{*+} \to D^0 \pi^+) = (49 \pm 8)\%$.

The cross sections obtained from our data are listed in Table 1, for decay modes (3) and (5) separately. The scaling cross section $s/\beta \cdot d\sigma/dx_E$ obtained by combining both decay channels is shown in Fig. 2a as a function of x_E. Our result is consistent with other cross section measurements [1–11], as well as the previous TASSO measurement [12]. The data from HRS [7] and PEP-4 [11] at $\sqrt{s} = 29$ GeV, which are up to now the statistically most precise published results at energies comparable to ours, have been rescaled using the recent branching ratios and are also shown in Fig. 2a for comparison. The error bars shown are statistical only. In addition systematic uncertainties due to the errors of the branching ratios used (11%), to the background subtraction (varying between 10% at low x_E and 4% at the highest x_E and depending on the decay channel), to the efficiency calculation (8%), and to the luminosity measurement (5%) have to be included.

All experiments find a broad energy spectrum of the D^{*+} mesons centered at x_E values around 0.6, compatible with the expected hard fragmentation of the charm quark [25]. The measurement therefore strongly supports the assumption that the

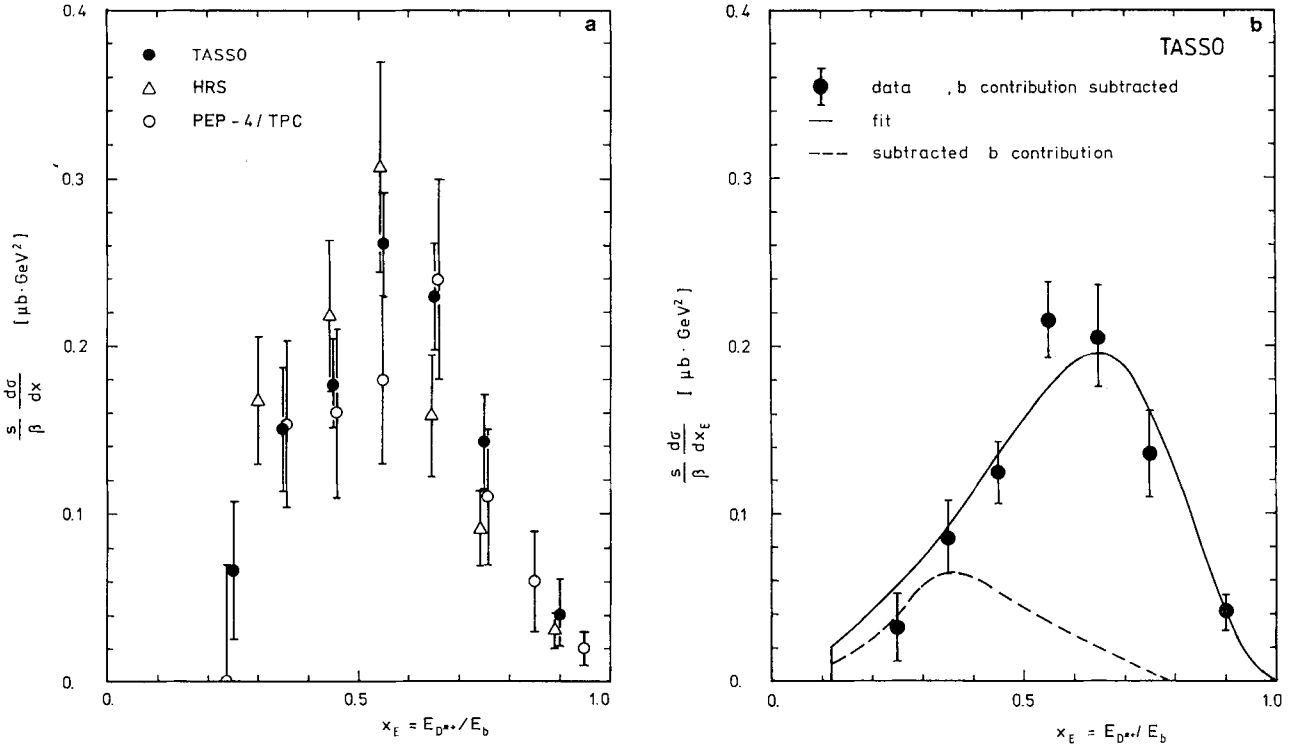

Fig. 2. a Scaled differential cross section $s/\beta\, d\sigma/dx$ for $e^+e^- \to D^{*\pm}X$, combining reactions (3) and (5). The errors shown are statistical only. The measurements of the HRS and PEP-4 collaborations at $\sqrt{s} = 29$ GeV are also shown for comparison. **b** Scaled differential cross section $s/\beta\, d\sigma/dx$ for $e^+e^- \to D^{*\pm}X$, after subtracting the contribution of B hadron decays to $D^{*\pm}$ mesons. Decay modes (3) and (5) are combined. The errors shown are statistical only. The solid curve represents the result of a fit to the fragmentation function proposed by [26]. The dashed curve shows the subtracted contribution from b decays

primary charm quark is contained in the charmed hadron.

The mean value of the fractional energy x_E of the D^{*+} mesons as calculated directly from our data is $\langle x_E \rangle = 0.55 \pm 0.02$. Integrating the measured differential cross section and extrapolating to the kinematical threshold, using the Lund Monte Carlo program, yielded the total cross section. The extrapolated part of the total cross section was 3%. For the ratio of the total cross section over the point cross section ($\sigma_{\mu\mu} = 66.3$ pb) at $\sqrt{\langle s \rangle} = 36.2$ GeV we obtained

$$R_{D^{*\pm}} = \frac{\sigma_{D^{*+}} + \sigma_{D^{*-}}}{\sigma_{\mu\mu}} = 1.28 \pm 0.09(\text{stat.}) \pm 0.18(\text{syst.}).$$

The errors include the experimental uncertainty, but not the uncertainties due to the branching ratios [24], which amount to ± 0.25. Assuming equal production rates for charged and neutral D^* mesons, the total D^* yield was found to be $R_{D^*} = 2R_{D^{*\pm}} = 2.56 \pm 0.18 \pm 0.36$.

Our data on the differential cross section extend to low x_E values where the decay of B hadrons to D^* mesons becomes important. We have calculated this contribution by using the Lund Monte Carlo program (the contribution corresponds to a branching ratio $B(B \to D^{*+} X) = 0.34$). The result is shown as the dashed curve in Fig. 2b. The scaling differential cross section after subtraction of the b quark component is presented in Fig. 2b. The mean value amounted to $\langle x_E \rangle_{\text{sub}} = 0.58 \pm 0.02$.

We have performed a fit to the data, after subtracting the b contribution, using the fragmentation function as proposed by [26]

$$f(x) \sim \left(x \left(1 - \frac{1}{x} - \frac{\varepsilon_x}{1-x} \right)^2 \right)^{-1}. \tag{6}$$

The fit yielded $\varepsilon_x = 0.19 \pm 0.03$ and is shown by the solid curve in Fig. 2b. The data are well described.

We want to emphasize that due to initial state photon radiation and gluon emission the mean of the fractional energy x_E is not equal to the mean of $z = (E + p_{\parallel})_h / (E + p)_q$, which was originally chosen as the scaling fragmentation variable (see e.g. [27] for a detailed study of these effects). To find the values of ε_z and $\langle z \rangle$ which correspond to the measured values ε_x and $\langle x_E \rangle_{\text{sub}}$, we used a Monte Carlo calculation based on the Lund program. The same functional form $f(z)$ has been employed to describe the fragmentation of the charm quark. We found that the values $\langle z \rangle = 0.69 \pm 0.03$ and $\varepsilon_z = 0.05$ gave the best description of the measured $D^{*\pm}$ cross section.

Using the same procedure as above for integration and extrapolation yields a total cross section for direct D^* production normalised to the point cross section of

$$R_{D^{*\pm}}(b \text{ subtracted}) = 1.02 \pm 0.07 \pm 0.18,$$

where in the systematic error an additional 10% uncertainty due to the b subtraction has been included. The total yield for direct production becomes $R_{D^*}(b \text{ subtracted}) = 2.04 \pm 0.14 \pm 0.35$. This value has to be compared with the expected total inclusive charm quark and antiquark yield of $R_{c,\bar{c}}(\text{primary}) \sim 2.8$ as calculated from the Quark Parton Model with 5% correction from QCD. The data thus indicate that the majority of the produced charm quarks fragment via D^* mesons. They are also consistent with a production ratio of vector mesons to pseudoscalar mesons of 3:1 in the charm sector. The result is also in agreement with previous measurements (see e.g. [28]).

The total cross section measurement can be used to determine the relative branching ratio of reactions (3) and (5). Above $x_E = 0.4$ the cross sections times branching ratios for the two channels are (1.39 ± 0.13) pb and (2.49 ± 0.26) pb, respectively. Thus the relative branching ratio is

$$\frac{B(D^0 \to K^- \pi^+ \pi^- \pi^+)}{B(D^0 \to K^- \pi^+)} = (1.79 \pm 0.36 \pm 0.27).$$

The systematic error includes the uncertainties of the acceptance calculation and the background subtraction. For comparison we quote the values measured by the ARGUS [10] $(2.17 \pm 0.28 \pm 0.23)$, MARK III [29] $(2.17 \pm 0.28 \pm 0.28)$, and CLEO [4] $(2.12 \pm 0.16 \pm 0.09)$ collaborations.

5 Measurement of the charm quark production asymmetry

5.1 Introduction

Two complementary methods were used to determine the charm quark production angular distribution. First we describe the well known method using the reconstructed D^* mesons. Then we discuss a measurement employing a method which does not at all rely on the explicit reconstruction of D^* mesons, but uses just the direction of the π_s^+ from the decay (1). This method was first applied recently by the HRS collaboration [30, 7]. Finally we combine both measurements for comparison with theory and other experiments.

In the standard model the interference between the photon and the Z^0 propagators is expected to produce a forward-backward asymmetry in the

production angular distribution of the primary charm quark. The asymmetry for $e^+e^- \to c\bar{c}$ is given in lowest order by

$$A_{c\bar{c}} = g_A^e g_A^c \frac{s m_Z^2}{m_Z^2 - s} \frac{3G_F}{4\sqrt{2}\pi\alpha e_c} \tag{7}$$

(if $m_Z^2 \gg s$). Here g_A^e, g_A^c are the electron and the charm quark axial vector coupling constants, $e_c = 2/3$ is the charge of the charm quark, G_F the Fermi coupling constant, and m_Z the Z^0 mass. In the standard model $g_A^e = -g_A^c = 1/2$.

5.2 *Measurement using reconstructed D^{*+} mesons*

The line of flight of the heavy charm quark can with good accuracy be approximated by the direction of the momentum of a high energy, charmed hadron (e.g. D^{*+} meson). For the determination of the angular distribution the data of channels (3) to (5) were combined. To further reduce the background, the following criteria were required in addition to those presented in Sect. 3: *i*) the momentum of each D^0 decay particle from reaction (3) and (4) must be greater than 1.0 GeV/c, *ii*) the fractional energy x_E of the D^{*+} candidate must be greater than 0.5, 0.5 and 0.6 for channels (3), (4), and (5) respectively. These criteria resulted in 214 $D^{*\pm}$candidates. The background has been estimated to be 16% with an estimated uncertainty of 3%.

The production angular distribution of the D^{*+} mesons is shown in Fig. 3a. The angle θ was defined as the polar angle between the incoming e^- and the outgoing D^{*+} containing the c quark (and not the $\bar{c}$ quark). The acceptance was found to be uniform over the polar angular range considered. A fit of the data to the function

$$\frac{1}{N}\frac{dN}{d\cos\theta} = k(1 + \cos^2\theta + a\cos\theta) \tag{8}$$

in the range $|\cos\theta| < 0.8$ yielded a measured asymmetry of $A = \frac{3}{8}a = -(0.166 \pm 0.075)$. The 16% background was assumed to be of the form $1 + \cos^2\theta$, and has been subtracted. Fitting (8) to a control region $0.16\ \text{GeV} < \Delta M < 0.20\ \text{GeV}$ resulted in $A = +(0.02 \pm 0.07)$, consistent with the expectation of $A = 0$. It was found that the result is only slightly dependent on the assumed background shape. Taking *i*) a constant background or *ii*) $1 + 3\cos^2\theta$ as the background parametrisation, changed the asymmetry by ± 0.004. Varying the background fraction by $\pm 3\%$ changed the result by ± 0.009. We take the combined value of ± 0.01 as the systematic uncertainty.

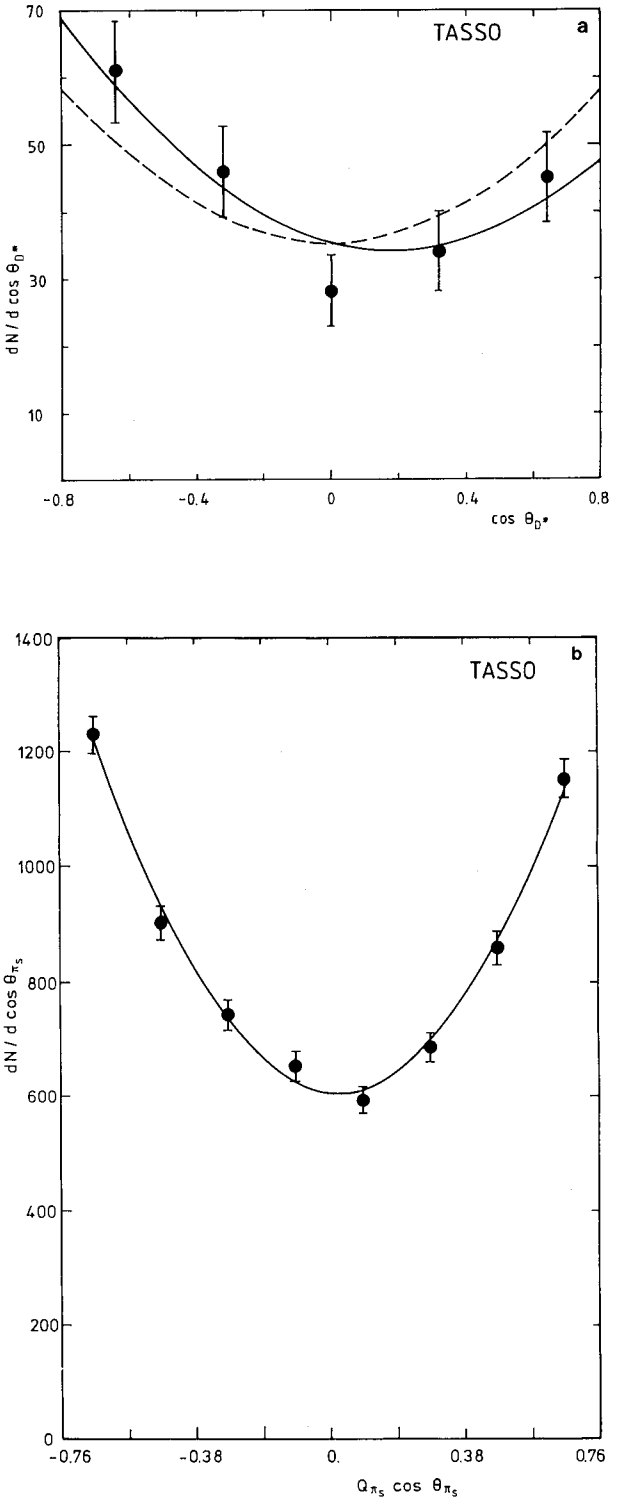

Fig. 3. a The D^{*+} production angular distribution for reactions (3) and (5) combined. θ is the angle between the directions of the incoming e^- and the outgoing $D^0\pi^+$ system. The solid curve represents the result of the fit described in the text. The dashed curve shows a forward-backward symmetric angular distribution proportional to $1 + \cos^2\theta$. **b** Charge weighted angular distribution of all tracks satisfying $p_T^2 < 0.0075\ (\text{GeV/c})^2$. The solid curve represents the result of the fit as described in the text

The result obtained so far has to be corrected for D^* mesons coming from bottom hadrons and higher order QED and QCD terms. Weak corrections are smaller and were neglected. It was found that D^{*+} mesons from the decay of B hadrons contribute $(5.0 \pm 1.5)\%$ to the data sample. The systematic uncertainty is due to the branching ratio of the decay $B \to D^{*+} X$ [31]. Subtracting this contribution reduces the measured asymmetry by $\Delta A = +0.008$. Higher order QED corrections and initial state bremsstrahlung change the asymmetry by $\Delta A = -0.01$. Thus, both effects change the measured value in the opposite direction to the b contribution. Higher order QCD corrections [32] amount to $\Delta A = +0.008$. The final value is $A = -(0.160 \pm 0.072 \pm 0.011)$. Using $m_Z = 92$ GeV in (7), the standard model predicts an asymmetry of $A_{GSW} = -0.157$ at $\sqrt{\langle s \rangle} = 36.2$ GeV. Thus the measurement is in agreement with the standard model prediction.

The result can be transformed into a measurement of the product of the axial vector coupling constants of the charm quark and the electron, which is a convenient variable for the comparison of results at different energies. From (7) we obtain $g_A^c g_A^e = -(0.255 \pm 0.116)$, where statistical and systematical errors have been added in quadrature.

5.3 *Measurement using low p_T pions*

This part of the analysis was performed with a restricted data sample in the c.m. energy range $32 \text{ GeV} < \sqrt{s} < 38 \text{ GeV}$, with a mean at 35.0 GeV, corresponding to an integrated luminosity of 185 pb^{-1}. In order to be statistically independent of the previous analysis, 192 events with a reconstructed $D^{*\pm}$ meson were removed. This resulted in a sample of 52,641 events with 91% of the data within the energy range between 34.5 and 35.5 GeV.

The charm quark angular distribution was measured using a sample of tracks enriched with π_s from reaction (1). The enrichment procedure relies on the small Q value of the decay and the hard fragmentation of the charm quarks. The latter means that the line of flight of the D^* meson should lie close to the jet axis. Because of its small transverse momentum with respect to the D^* line of flight this is also true for the π_s. Thus a cut on the p_T^2 of a track with respect to the jet axis can be used to enrich the track sample with π_s mesons.

The thrust axis calculated using all charged tracks in an event was taken as the jet axis. A thrust cut of $T > 0.9$ was applied to remove events with hard gluon radiation. The latter weakens the correlation between the D^* line of flight and the thrust axis, broadening the p_T^2 distribution of the π_s. Candidate tracks were required to have momenta, corrected for ionisation loss, in the range $0.5 < p < 1.2$ GeV/c and to have polar angles within $|\cos\theta| < 0.76$. The latter requirement was chosen to minimise acceptance effects. The high momentum cut removes tracks which are too energetic to be π_s candidates while the low momentum cut reduces backgrounds from soft fragmentation tracks and π_s in $b\bar{b}$ events (which have a softer momentum spectrum). 94,795 tracks passed these cuts. The p_T^2 spectrum of the candidate tracks, as calculated with respect to the thrust axis, is shown in Fig. 4.

The method relies on an adequate understanding of the distributions of both the low p_T^2 signal and the background from tracks not coming directly from $D^{*\pm}$ mesons. Therefore, we need to prove that Monte Carlo simulations of non-charm events cannot produce such a peak within plausible ranges of tuning

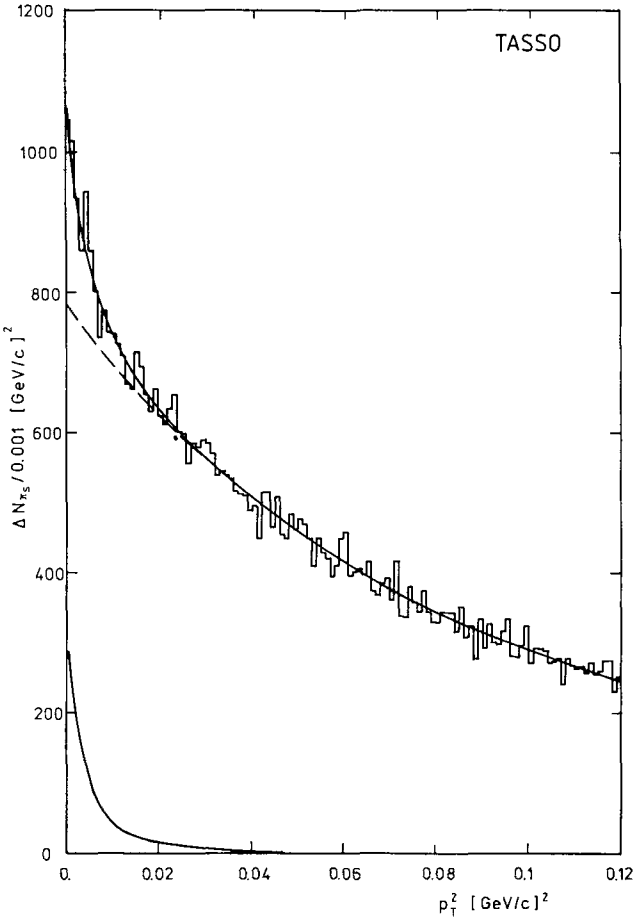

Fig. 4. Distribution of the transverse momentum squared of all particles with respect to the thrust axis. Superimposed is the result from a fit as described in the text. The contributions of the signal and the background components are also shown separately

parameters. Furthermore, the effect of uncertainties in the parametrisation of the signal shape needs to be quantified.

In order to determine the number of π_s in the track sample the shape of the p_T^2 spectrum of π_s mesons was parametrised by the function

$$S(p_T^2) \sim N_S(e^{-Ap_T^2} + Ce^{-Bp_T^2}) \tag{9}$$

where N_S is the number of π_s candidates. The values of the constants A, B and C were found by fitting the p_T^2 spectrum of π_s in Monte Carlo events in which a full detector simulation had been performed. Three different Monte Carlo models were used: the Lund Monte Carlo versions 6.2 [23] (2nd order QCD matrix element and string fragmentation) and 6.3 [33] (parton shower), and an independent jet fragmentation model incorporating the extended FKSS calculation of full second order QCD matrix elements (henceforth referred to as QCDFF [34]).

As a check, the three parameter sets obtained from the different Monte Carlo calculations were used to fit the p_T^2 spectrum of π_s from 149 fully reconstructed $D^{*\pm}$ mesons from reactions (3) and (4) (estimated background of 15%). With N_S as the only free parameter, we obtained a χ^2 of 13.2 (QCDFF), 16.6 (Lund 6.3), and 18.1 (Lund 6.2) for 24 degrees of freedom. The results of the fits are shown in Fig. 5a to c. All three signal shapes were considered to give a good description of the data. Note that the final measured asymmetry was almost insensitive to the variation of the signal shape given by the different Monte Carlo models.

The p_T^2 distribution of the overall track sample was then fitted in the range $p_T^2 < 0.24\ (\mathrm{GeV/c})^2$ with one of the above Monte Carlo signal shapes plus a smooth background shape. The background term was parametrised as

$$B_1(p_T^2) \sim \frac{N_B}{1 + \alpha p_T^2 + \beta p_T^4}. \tag{10}$$

The signal size (N_S) and the background shape and size (N_B, α and β) were parameters of the fit.

As a check, this parametrisation has been used also to fit the p_T^2 spectra of each of the three Monte Carlo data sets. Within the accuracy of these fits the obtained numbers of π_s were in agreement with the expectation. However, none of the parameter sets (α, β) of the Monte Carlo calculations described the background shape of the data well. Monte Carlo tests showed that a peak could not be produced at low p_T^2 by contrived parametrisation without making drastic changes in other, well-measured event characteristics. For example, a quantity sensitive to the p_T^2 distribution is the event sphericity, which is one of the variables on which the Monte Carlo is tuned.

We therefore chose a background parametrisation according to (10), allowing also α and β to vary during the fit. Each of the three Monte Carlo signal shapes have been used with the background parametrisation B_1 to estimate the π_s content of the p_T^2 spectrum of the data. The result of the fit using the QCDFF signal shape is superimposed on Fig. 4 with the signal and background contributions separated. The sum of both

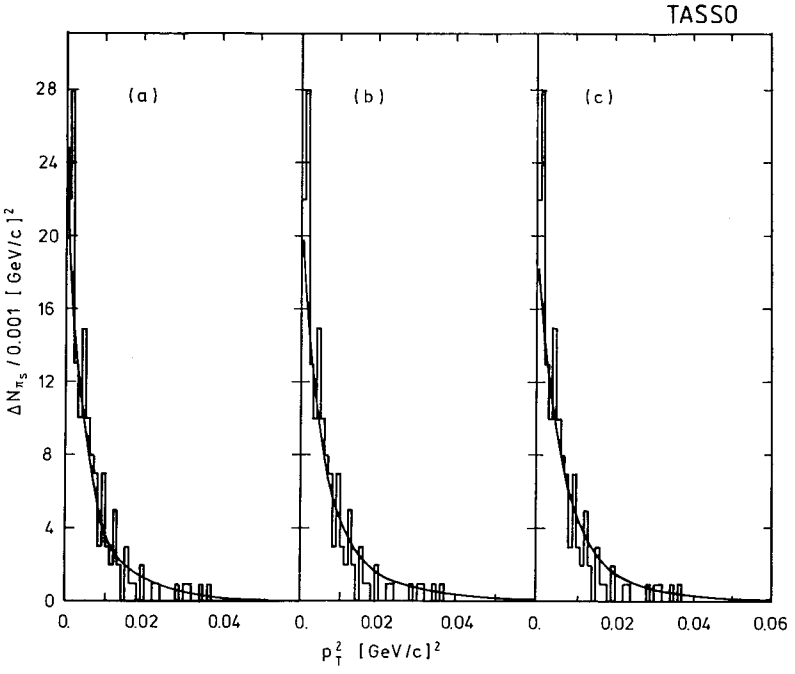

Fig. 5a–c. Distribution of the transverse momentum squared with respect to the thrust axis for π_s mesons from reconstructed $D^{*\pm}$ decays. Superimposed is the predicted signal shape from three different Monte Carlo calculations **a**) a 2nd order QCD calculation with independent jet fragmentation (QCDFF), **b**) Lund Monte Carlo version 6.2, and **c**) Lund Monte Carlo version 6.3

contributions describes the data well. Choosing a cut of $p_T^2 < 0.0075\ (\mathrm{GeV/c})^2$, which maximises the sensitivity to the asymmetry for the signal and background sizes obtained, the three fits gave signal sizes of $N_S = 1189 \pm 91$ (QCDFF), $N_S = 1373 \pm 103$ (Lund 6.3) and $N_S = 1409 \pm 106$ (Lund 6.2). The weighted mean of $1310 \pm 99 \pm 100$ was taken as the signal estimate, where the systematic error is the spread of the three results. This corresponds to a purity of the track sample of $(21 \pm 2)\%$.

To measure the asymmetry from the track sample, the charge-weighted angular distribution ($Q \cos\theta$) of the tracks was calculated, where Q is the charge of the track. The angular distribution, shown in Fig. 3b, was then fitted by the sum of eq. (8) and a background contribution of the form $l(1 + b\cos^2\theta)$. The normalisation k was fixed corresponding to the measured number of π_s, and the background normalisation l and the shape parameter b were left free. The result of this fit is shown as the curve in Fig. 3b.

The fit yielded a value of $A = \frac{3}{8}a = -(0.184 \pm 0.050)$, with $\chi^2 = 3.25$ for 5 degrees of freedom, where the error is from variance of the fitted parameter a. Combined with the uncertainty on the signal size this gives $A = -(0.184 \pm 0.052 \pm 0.014)$. The systematic error due to varying the value of b was estimated to be less than ± 0.001 and ignored.

The procedure was repeated *i)* using tracks in the momentum range $1.5 < p < 3.5$ GeV/c (beyond the kinematic limit for π_s) and *ii)* using tracks of $0.02 < p_T^2 < 0.028\ (\mathrm{GeV/c})^2$ (outside the signal region). In both cases the product ka was examined as k was not determined for these samples. The high momentum sample yielded $ka = -(1.8 \pm 1.9)$ for $p_T^2 < 0.025\ (\mathrm{GeV/c})^2$ and $ka = -(0.22 \pm 0.85)$ for $p_T^2 < 0.005\ (\mathrm{GeV/c})^2$, while the high p_T^2 sample yielded $ka = -(0.4 \pm 1.6)$. All values were consistent with no asymmetry. Fitting the angular distribution without charge weighting gave a value of $a = -(0.042 \pm 0.049)$ for $p_T^2 < 0.0075\ (\mathrm{GeV/c})^2$, again consistent with zero.

Systematic errors in the signal and background size estimates were examined using two methods. First the above procedure was repeated using a different form of the background shape,

$$B_2(p_T^2) \sim N_B(e^{-\gamma p_T^2} + \kappa)$$

for all three signal shapes. Secondly the signal size was estimated by fitting the background shape alone to the high p_T^2 region of the data. The lower limit for the p_T^2 region fitted was varied in the range 0.025 to $0.06\ (\mathrm{GeV/c})^2$. This range was constrained by the requirement that there be little signal in the background region and by the loss of sensitivity to the background shape at large values of the cut. The fitted background shape was then used to estimate the signal in the low p_T^2 region. This technique was repeated using both background forms. In all cases the signal estimates were consistent with those used in the analysis.

The variation in the measured asymmetry was checked in both the data and Monte Carlo samples for systematic dependencies on the cuts applied, particularly that on p_T^2. The observed shifts were found to be consistent within statistics. Therefore we are confident that any such systematic effect is small compared to the statistical uncertainty and assign a systematic error of ± 0.026.

Using a Monte Carlo simulation and the CLEO measurement of $B \to D^{*\pm} X$ decays [31] it was estimated that the track sample included $74^{+29}_{-22}\ \pi_s$ mesons from $b\bar{b}$ events which resulted in a shift of $\Delta A = +(0.017 \pm 0.009)$. Correcting for higher order QED and QCD processes gave shifts of $\Delta A = -0.01$ and $\Delta A = +0.009$, respectively. Applying all corrections and combining the errors leads to a final asymmetry of $A = -(0.168 \pm 0.047 \pm 0.027)$, which again is in agreement with the standard model prediction of $A_{GSW} = -0.145$ for $\sqrt{\langle s \rangle} = 35$ GeV and $m_Z = 92$ GeV. This in turn yields a value for the product of the coupling constants of $g_A^e g_A^c = -(0.290 \pm 0.093)$, where the errors have been added in quadrature.

5.4 *Final result*

Since the two analyses have used different sets of $D^{*\pm}$ events their results are statistically independent. Also the dominant sources of systematic uncertainties differ in the two cases, so that the results for the product of the coupling constants can be averaged to yield

$$g_A^e g_A^c = -(0.276 \pm 0.073).$$

The statistical and systematic uncertainties for each measurement have been added in quadrature before combination. This result is in good agreement with the standard model prediction of $g_A^e g_A^c = (-\frac{1}{2})(\frac{1}{2}) = -\frac{1}{4}$ and with previous experimental results [7, 35].

6 Test of flavour independence of α_s

A measurement of the energy-energy correlation (EEC) in e^+e^- annihilation can be used to test perturbative QCD. In contrast to other variables like thrust it has the advantage that no jet definition is

necessary, thus avoiding difficulties in distinguishing events with three or more jets from two-jet events. Of particular interest is the average normalised EEC, defined as [34, 36, 37]

$$\frac{1}{\sigma_0}\frac{d\Sigma(\cos\chi)}{d\cos\chi}=f(\cos\chi)=\frac{1}{N_{\text{ev}}}\sum_{\text{Events}}\sum_{i,j}\frac{E_iE_j}{W_{\text{vis}}^2}\delta(\cos\chi-\cos\chi_{ij}), \tag{11}$$

where χ_{ij} is the angle between two charged particles i and j with energies E_i and E_j, respectively. The summations extend over all pairs i,j of particles in an event including the case $i=j$, and over all events N_{ev}. W_{vis} is the total visible energy of the event.

The normalisation is such that

$$\int f(\cos\chi)\,d\cos\chi=1. \tag{12}$$

QCD predicts that at high energies the correlation around $\cos\chi=0$ is dominated by single hard gluon bremsstrahlung and is therefore proportional to the quark gluon coupling constant α_s. The effects of gluon emission are enhanced, and those of centre of mass energy dependence and fragmentation are minimised, if instead the forward-backward asymmetry of the EEC (denoted AEEC)

$$A(\cos\chi)=f(\cos(\pi-\chi))-f(\cos\chi) \tag{13}$$

is used. Remaining effects due to fragmentation near $|\cos\chi|\sim 1$ can be further reduced by constraining the fits to obtain α_s to the region $|\cos\chi|<0.7$ of the asymmetry.

The coupling constant was determined by comparing the data with Monte Carlo events which have been traced through a full detector simulation. We chose to use the QCDFF Monte Carlo for this comparison [34]. In general many different samples of Monte Carlo events have to be processed to properly account for the effects of different values of α_s. To avoid this, an event weighting procedure was devised. Let

$$r=\frac{\alpha_s(\text{to be simulated})}{\alpha_s(\text{generated})},$$

then each four-parton event received a weight r^2, each three-parton event a weight $r+T_{21}r^2$ (T_{21} was the ratio of average 2nd and 1st order contributions to three-parton final states), and each two-parton event a weight equal to the fractional two-parton cross section. The procedure was extensively tested, and it was found that the uncertainty introduced by this method results in a possible variation of the measured α_s value of at most ± 0.006 for $0.1<\alpha_s<0.2$.

The event weighting procedure was first applied to the total hadronic sample assuming the same α_s value for all flavours in the Monte Carlo. The AEEC distribution was fitted in the region $|\cos\chi|<0.7$, yielding $\alpha_s(all)=0.149\pm 0.004$ with a $\chi^2/\text{d.o.f.}=4.6/6$. By varying the range between $|\cos\chi|<0.6$ and $|\cos\chi|<0.8$ the value of α_s changed by ± 0.006. This result is consistent with a more detailed study of energy-energy correlations in our data [36].

The AEEC distribution of the reconstructed $D^{*\pm}$ sample (shown in Fig. 6) was then fitted in the same $|\cos\chi|$ range, but fixing the α_s value for u, d, s and b flavours to the average of all hadrons (including c flavour), and allowing only $\alpha_s(c)$ to vary. The result obtained is $\alpha_s(c)=0.135\pm 0.056$ with a $\chi^2/\text{d.o.f.}=3.8/6$. A variation of the $|\cos\chi|$ range as above resulted in a change of ± 0.015 of the $\alpha_s(c)$ value. The Monte Carlo distribution (also shown in Fig. 6)

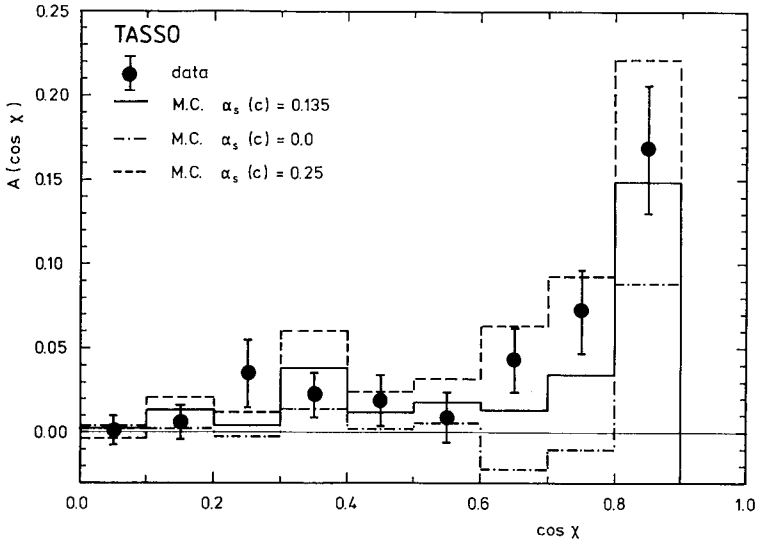

Fig. 6. Energy-energy correlation asymmetry distribution for the tagged charm sample. The solid curve represents the QCDFF Monte Carlo expectation for the best fit of $\alpha_s(c)$

describes the data reasonably well. Most of the systematic uncertainties are expected to cancel in the ratio of $\alpha_s(c)$ to $\alpha_s(all)$. We found for this ratio $R = \alpha_s(c)/\alpha_s(all) = 0.91 \pm 0.38$.

Several sources of systematic errors have been investigated. *i*) Varying the $|\cos\chi|$ range, as described above, yielded a significant effect only in the fit to the D^* sample, corresponding to a change in R of ± 0.10. *ii*) A variation of the assumed $\alpha_s(all)$ value by ± 0.01 changed R by ± 0.02. *iii*) Varying the fraction of charm events in the $D^{*\pm}$ sample by $\pm 3\%$ resulted in a change of ± 0.01 in the ratio R. *iv*) The influence of the fragmentation of the charm quark has been investigated by comparing two different Monte Carlo calculations: the QCDFF Monte Carlo which has been used to obtain the above values and the Lund Monte Carlo. Any deviation between these two calculations is considered as a proper measure for the systematic error due to the different fragmentation schemes. In this error we also include any present uncertainty of the parameter $\langle z \rangle$ (or in case of an underlying Peterson et al. distribution of ε_z). Because this variable presently is known quite precisely [27], this error is expected to be small. We found that we have to attribute an error of ± 0.11 on the ratio R to account for these effects. Combining all the systematic errors in quadrature we find as our final result

$$\frac{\alpha_s(c)}{\alpha_s(all)} = 0.91 \pm 0.38 \pm 0.15.$$

This result is in agreement with our previous measurement, using a different technique [14]. Comparing this measurement with our recent result concerning the strong coupling of the b quark [34], leads to the conclusion that no violations of flavour independence of the strong coupling constant has been found in our experiment.

7 Measurement of the D^0 lifetime

The large amount of data taken in 1986 during the last year of PETRA operation (31,176 hadronic events, corresponding to $110\,\mathrm{pb}^{-1}$) allowed us to improve significantly our previous measurement (8,608 events, $49.5\,\mathrm{pb}^{-1}$) of the D^0 lifetime [15,38]. The method of analysis did not change substantially and is repeated only briefly here. The neutral D mesons were identified in the decay (1), with the subsequent decays (3) and (4). Events containing these decays were selected anew using tracks which had information from all three chambers which comprise the TASSO inner detector: the vertex chamber, the inner proportional chamber, and the central drift chamber. To ensure that the tracks had been reliably reconstructed in the vertex chamber, only tracks with at least 4 of 8 possible vertex detector hits and a χ^2 per degree of freedom of less than 2.5 for reconstructing the entire track in the plane perpendicular to the beam were accepted. In other respects the selection criteria were the same as above, except that *i*) two particle combinations were formed only among the tracks in the same hemisphere, as defined by the sphericity axis, and *ii*) for decay mode (4) only tracks of momentum greater than 1.4 GeV/c were used.

The combinations accepted so far were geometrically fitted to a common vertex [39], and those ascribed to reaction (3) in addition kinematically constrained to the D^0 mass [40]. Candidates with badly reconstructed decay vertices or with a $\chi^2 > 5.0$ for the kinematic constraint were removed. The other combinations were paired with each charged track in the same hemisphere to form D^* candidates.

We found 29 events of mode (3) and 19 events in mode (4) which fulfill $\Delta M < 0.15$ GeV and $x_E > 0.5$. The background was estimated by Monte Carlo methods to be about 5% and 15% respectively. Furthermore two decays from mode (4) were removed because the event topology was consistent with tau pair production.

To determine the decay distance of the D^0 mesons we followed closely our previous analysis [15]. The decay distances were converted into proper times using $c\tau_i = \frac{l_i}{\beta\gamma}$, $\gamma\beta = p_{D^0}/M_{D^0}$.

For the S^0 decay mode a compensation is necessary for the unseen energy of the missing π^0. This has been accomplished by using $\gamma\beta = p(K^-\pi^+)/M(K^-\pi^+)$. Monte Carlo calculations showed that this approximation introduces an additional uncertainty for i of less than 6%.

The distribution of the measured proper decay times weighted by their errors is shown in Fig. 7, where the data from our previous analysis are included (yielding totally 60 reconstructed vertices). The D^0 lifetime was extracted applying a maximum likelihood fit to this data sample yielding $\tau_{D^0} = (4.8^{+1.0}_{-0.9}) \cdot 10^{-13}$ s. This value was used to produce the curve superimposed on Fig. 7.

To show that the analysis procedure caused no systematic shifts towards positive or negative lifetimes, events were selected from the upper D^0 side band and then analysed in the same way as the data, except that no kinematic fit was performed. A maximum likelihood fit resulted in an average lifetime of $(0.03 \pm 0.20) \cdot 10^{-13}$ s.

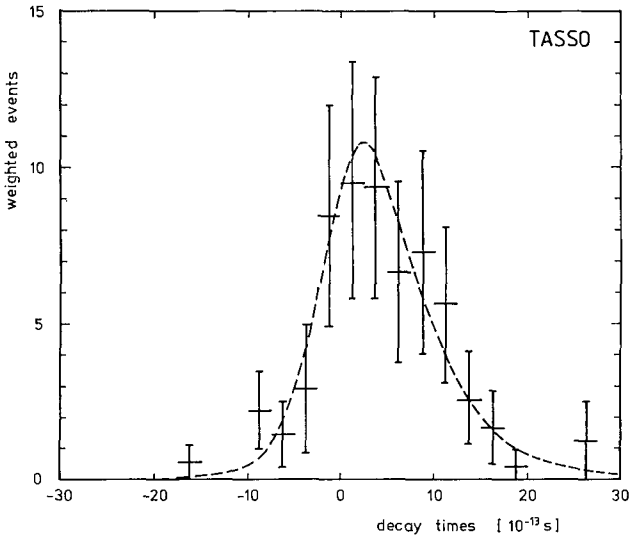

Fig. 7. The weighted distribution of the proper decay times of the 60 reconstructed D^0 mesons. The curve was produced with the D^0 lifetime found in the maximum likelihood fit

Several sources of systematic errors have been examined. *i*) A variation of the assumed vertex detector resolution by $\pm 20\%$ changed the value of the lifetime by $\pm 0.3 \cdot 10^{-13}$ s. Another way to check the correct resolution function is to introduce a second free parameter into the maximum likelihood fit which multiplies the error of each measurement. Fitting both the lifetime and this scale factor decreased the value of τ_{D^0} by $-0.6 \cdot 10^{-13}$ s, the resulting scale factor being compatible with unity. To be as conservative as possible we allowed a shift of $-0.6 \cdot 10^{-13}$ s for the D^0 lifetime. *ii*) Varying the size of the beam spot by $\pm 20\%$ changed the lifetime by less than $\pm 0.1 \cdot 10^{-13}$ s. *iii*) A change of 100 μm in the vertical alignment of the vertex chamber with respect to the central drift chamber gave rise to a change in τ_{D^0} of about $\pm 0.1 \cdot 10^{-13}$ s. *iv*) Varying the assumed B lifetime by as much as $\pm 50\%$ changed the D^0 lifetime by $\pm 0.1 \cdot 10^{-13}$ s. *v*) The value of τ_{D^0} is changed by $\pm 0.2 \cdot 10^{-13}$ s if the fraction of accepted D^0 mesons from B meson decay was varied between 1.5% and 7.0%. *vi*) Varying the assumed background fractions by $\pm 50\%$ of their values changed the lifetime by $\pm 0.2 \cdot 10^{-13}$ s. Adding all effects in quadrature we obtained a systematic error of $^{+0.5}_{-0.7} \cdot 10^{-13}$ s.

Our final result for the D^0 lifetime is

$$\tau_{D^0} = (4.8^{+1.0+0.5}_{-0.9-0.7}) \cdot 10^{-13} \text{ s},$$

in good agreement with our previous analysis [15] and other experiments [24].

8 Summary

We have studied $D^{*\pm}$ charm meson production at centre of mass energies between 28 and 46.8 GeV. We found a hard fragmentation distribution of the $D^{*\pm}$ mesons, with a mean value of $\langle x_E \rangle = 0.55 \pm 0.02$. The total cross section normalised to the point cross section was measured to be $R(D^{*\pm}) = 1.28 \pm 0.09 \pm 0.18$. The $D^{*\pm}$ angular distribution shows a forward-backward asymmetry, indicating the presence of a weak neutral current contribution to $e^+e^- \to c\bar{c}$. The product of the axialvector couplings of the electron and the charm quark to the Z^0 was determined by two complementary methods to be $g_A^e g_A^c = -(0.276 \pm 0.073)$ in agreement with the standard model prediction of -0.25. Using a sample of reconstructed $D^{*\pm}$ mesons we have investigated the influence of the quark flavour on the strong coupling between quarks and gluons. We found the ratio of the strong coupling constants for charm jets to average jets consistent with unity, indicating that the strong interaction is flavour independent. Finally we presented an update of a D^0 lifetime measurement and found a value of $\tau_{D^0} = (4.8^{+1.0+0.5}_{-0.9-0.7}) 10^{-13}$ s, in agreement with previous measurements.

Acknowledgements. We gratefully acknowledge the efforts of the PETRA machine group for high-luminosity running, and the DESY directorate for their support. Those of us from abroad wish to thank the DESY directorate for their hospitality extended to us while working at DESY.

References

1. MARK II Coll. J.M. Yelton et al.: Phys. Rev. Lett. 49 (1982) 430
2. CLEO Coll. C. Bebek et al.: Phys. Rev. Lett. 49 (1982) 610
3. CLEO Coll. P. Avery et al.: Phys. Rev. Lett. 51 (1983) 1139
4. CLEO Coll. D. Bortoletto et al.: Phys. Rev. D37 (1988) 1719
5. HRS Coll. S. Ahlen et al.: Phys. Rev. Lett. 51 (1983) 1147
6. HRS Coll. M. Derrick et al.: Phys. Lett. 146B (1984) 261
7. HRS Coll. P. Baringer et al.: Phys. Lett. 206B (1988) 551
8. JADE Coll. W. Bartel et al.: Phys. Lett. 146B (1984) 121
9. DELCO Coll. H. Yamamoto et al.: Phys. Rev. Lett. 54 (1985) 522
10. ARGUS Coll. H. Albrecht et al.: Phys. Lett. 150B (1985) 235
11. PEP-4/TPC Coll. H. Aihara et al.: Phys. Rev. D34 (1986) 1945
12. TASSO Coll. M. Althoff et al.: Phys. Lett. 126B (1983) 493
13. TASSO Coll. M. Althoff et al.: Phys. Lett. 135B (1984) 243
14. TASSO Coll. M. Althoff et al.: Phys. Lett. 138B (1984) 317
15. TASSO Coll. M. Althoff et al.: Z. Phys. C – Particles and Fields 32 (1986) 343
16. TASSO Coll. R. Brandelik et al.: Phys. Lett. 83B (1979) 261
17. TASSO Coll. R. Brandelik et al.: Z. Phys. C – Particles and Fields 4 (1980) 87
18. TASSO Coll. R. Brandelik et al.: Phys. Lett. 114B (1982) 65
19. D.M. Binnie et al.: Nucl. Instrum. Methods 228 (1985) 267
20. S. Nussinov: Phys. Rev. Lett. 35 (1976) 1672
21. G.J. Feldman et al.: Phys. Rev. Lett. 38 (1977) 1313

22. G. Goldhaber: Proceedings of the XVIII Rencontre de Moriond, La Plagne 1983, Vol. 2, p. 137
23. T. Sjöstrand: Comput. Phys. Commun. 39 (1986) 347
24. Particle Data Group M. Aguilar-Benitez et al.: Phys. Lett. 204 B (1988) 1
25. M.G. Bowler: Z. Phys. C – Particles and Fields 11 (1981) 169
26. C. Peterson et al.: Phys. Rev. D 27 (1983) 105
27. S. Bethke: Z. Phys. C – Particles and Fields 29 (1985) 175
28. P. Mättig: Phys. Rep. 177 (1989) 141
29. MARK III Coll. J. Adler et al.: Phys. Rev. Lett. 60 (1988) 89
30. HRS Coll. S. Abachi et al.: Phys. Lett. 205 B (1988) 411
31. CLEO Coll. D. Bortoletto et al.: Phys. Rev. D 35 (1987) 19
32. J. Jersák, E. Laermann, P.M. Zerwas: Phys. Lett. 98 B (1981) 363
33. T. Sjöstrand, M. Bengtsson: Comput. Phys. Commun. 43 (1987) 367
34. TASSO Coll. W. Braunschweig et al.: Z. Phys. C – Particles and Fields 42 (1989) 17
35. S.L. Wu: e^+e^- Interactions at High Energies, 1987 Int. Symp. on Lepton-Photon Int. at High Energies (Hamburg), Nucl. Phys. B 3 (Proc. Suppl.) (1988) 39
36. TASSO Coll. W. Braunschweig et al.: Z. Phys. C – Particles and Fields 36 (1987) 349
37. A. Ali, F. Barreiro: Phys. Lett. 118 B (1982) 155
38. D. Strom: Ph.D. thesis, Univ. of Wisconsin, Madison (1986)
39. D.H. Saxon: Nucl. Instrum. Methods A 234 (1985) 258
40. G.E. Forden, D.H. Saxon: Nucl. Instrum. Methods A 248 (1986) 439